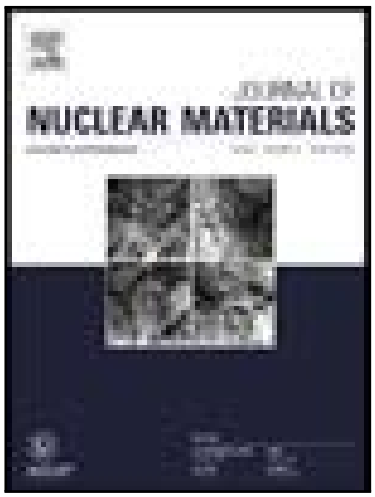

Neutron Irradiation Tolerance of Potassium-Doped and Rhenium-Alloyed Tungsten

Shuhei Nogami , Dmitry Terentyev , Aleksandr Zinovev , Chao Yin , Michael Rieth , Gerald Pintsuk , Akira Hasegawa

PII: S0022-3115(21)00232-4
DOI: https://doi.org/10.1016/j.jnucmat.2021.153009
Reference: NUMA 153009

To appear in: *Journal of Nuclear Materials*

Received date: 18 January 2021
Revised date: 26 March 2021
Accepted date: 8 April 2021

Please cite this article as: Shuhei Nogami , Dmitry Terentyev , Aleksandr Zinovev , Chao Yin , Michael Rieth , Gerald Pintsuk , Akira Hasegawa , Neutron Irradiation Tolerance of Potassium-Doped and Rhenium-Alloyed Tungsten, *Journal of Nuclear Materials* (2021), doi: https://doi.org/10.1016/j.jnucmat.2021.153009

Neutron Irradiation Tolerance of Potassium-Doped and Rhenium-Alloyed Tungsten

Shuhei Nogami[1], Dmitry Terentyev[2], Aleksandr Zinovev[2], Chao Yin[2], Michael Rieth[3], Gerald Pintsuk[4], Akira Hasegawa[1]

[1] Department of Quantum Science and Energy Engineering, Graduate School of Engineering, Tohoku University, 6-6-01-2, Aramaki-aza-Aoba, Aoba-ku, Sendai 980-8579, Japan

[2] Structural Materials Group, Institute of Nuclear Materials Science, SCK·CEN, 2400 Mol, Belgium

[3] Institute for Applied Materials, Karlsruhe Institute of Technology, Hermann-von-Helmholtz-Platz 1, 76344 Eggenstein-Leopoldshafen, Germany

[4] Forschungszentrum Jülich GmbH, Institute for Energy and Climate Research, 52425 Jülich, Germany

Corresponding Author

Name Shuhei Nogami

Postal address Department of Quantum Science and Energy Engineering, Graduate School of Engineering, Tohoku University, 6-6-01-2, Aramaki-aza-Aoba, Aoba-ku, Sendai 980-8579, Japan

Telephone +81-22-795-7923

Fax number +81-22-795-7924

E-mail address shuhei.nogami.d3@tohoku.ac.jp

Abstract

Tungsten (W) based materials for fusion reactor applications have been developed in Japan for the last decade to improve thermo-mechanical properties and tolerance with respect to neutron-irradiation effects. Potassium (K) doping for dispersion strengthening and alloying by rhenium (Re) for solid solute softening and strengthening were applied to W fabricated by powder metallurgy. Thereby modified W materials, e.g. K-doped W and K-doped W-3%Re, demonstrated a higher recrystallization temperature threshold, an increase in strength and ductility, and a reduction in ductile-to-brittle transition temperature (DBTT) compared to pure W in the non-irradiated state. Embrittlement caused by displacement damage and its amplification due to solid transmutation products is expected to be an intrinsic issue of W based materials under neutron irradiation environment inherent to future fusion reactors. In this paper, the effect of K-doping and alloying by Re on the neutron-irradiation-induced embrittlement of W was investigated at neutron fluence causing a considerable amount of solid transmutation products.

Keywords:

Tungsten, Potassium doping, Alloying by rhenium, Neutron irradiation, Embrittlement

1. Introduction

Embrittlement caused by displacement damage and its enhancement due to solid transmutation products are intrinsic issue of tungsten (W) based materials under neutron irradiation environment of future fusion reactors. According to the open literature, W based materials showed increase in strength (irradiation hardening), decrease in ductility, and increase in ductile-to-brittle transition temperature (DBTT) due to neutron irradiation, as do most of the metals [1–4].

W based materials for fusion reactor applications with improved thermo-mechanical properties and neutron-irradiation tolerance have been developed in Japan for the last decade. Potassium (K) doping for dispersion strengthening and alloying by rhenium (Re) for solid solute softening and strengthening were applied to W fabricated by a powder metallurgy [5–16]. As examples of improved thermo-mechanical properties in the non-irradiated state, hot-rolled plates of K-doped W, W-3%Re, and K-doped W-3%Re showed higher recrystallization temperature, increase in strength and ductility, and decrease in DBTT compared to pure W [5, 6, 9, 11–16]. In addition to the properties in the non-irradiated state, neutron-irradiation tolerance of these materials was shown by the collaboration project by Japan and the U.S.A., called PHENIX (2013–2018). Therein, neutron irradiation tests at displacement damage ranging from 0.40 to 0.74 dpa at irradiation temperature ranging from 570 to 1020 ºC were performed in the High Flux Isotope Reactor (HFIR) of Oak Ridge National Laboratory (ORNL) in the U.S.A. using thermal neutron shielding to suppress irradiation by thermal neutrons [17–19]. As a positive result of K-doping and Re-addition, total elongation in tensile test of K-doped W, W-3%Re, and K-doped W-3%Re remained after neutron irradiation, where pure W showed complete loss of ductility.

The neutron irradiation study in the above-mentioned PHENIX project did not investigate the effects of simultaneous solid transmutation. In contrast, displacement damage

will reach a level in a future fusion DEMO reactor and beyond, where the solid transmutation cannot not be regarded as negligible. According to Bolt et al., the amounts of displacement damage and transmutant Re produced in W of the first wall and divertor of a DEMO-like fusion power reactor after 5 years of operation were 30 dpa and 6% and 15 dpa and 3%, respectively [20, 21]. Irradiation hardening of pure W increased with increase in displacement damage up to approximately 0.5 dpa. Above this damage level, saturation of irradiation hardening was observed if thermal neutron irradiation was suppressed, whereas significantly higher irradiation hardening was produced if accompanied by thermal neutron irradiation. Thermal neutrons could cause solid transmutations via (n, γ) neutron capture reactions, resulting in accumulation of Re, osmium (Os), and tantalum (Ta), which could result in the formation of precipitates and clusters in W, inducing significant irradiation hardening [22–37].

In this paper, mechanical property changes of K-doped W and K-doped W-3%Re caused by neutron irradiation is summarized, where displacement damage was above the mentioned saturation level accompanied by solid transmutation from W to Re and Os. A commercially available pure W fulfilling the ITER-specifications has been added in the present study to assess the effect of K-doping and alloying by Re on the neutron-irradiation-induced embrittlement.

2. Experimental

2.1 Materials

To evaluate the effects of K-doping and alloying by Re, K-doped W and K-doped W-3%Re plates (7 mm thick), supplied by A.L.M.T. corp. in Japan, were examined in the present study, which were fabricated by powder metallurgy and unidirectional hot rolling followed by a stress relief heat treatment. The manufacturing details and thermo-mechanical

properties in the non-irradiated state of these materials were described in open literature [5, 6, 9, 11–13, 15, 16]. The concentration of K in these materials was approximately 30 ppm. Due to the fabrication method using unidirectional rolling, grains of K-doped W and K-doped W-3%Re exhibited a pancake-like shape.

In addition to the K-doped W and K-doped W-3%Re plates, pure W rod with a square cross-section (35 mm × 35 mm cross section), supplied by PLANSEE AG in Austria, was also examined for a purpose of comparison. The material was fabricated by powder metallurgy and final product in a form of bar was forged on two sides followed by a stress relief heat treatment (hereafter, this material is referred to as IGP pure W standing for ITER specification Plansee pure W). The details and thermo-mechanical properties in the non-irradiated state of this material were described in open literature [38–42]. Due to the fabrication method using forging on two sides, grains of IGP pure W have a carrot-like shape.

The content of interstitial impurities (carbon (C), oxygen (O), and nitrogen (N)), grain sizes along L, T, and S directions, which were determined by high angle grain boundaries (HAGBs), and ultimate tensile strength at 300 and 500 ºC along L direction of IGP pure W, K-doped W, and K-doped W-3%Re are summarized in Table 1 [13, 15, 16, 38–42]. Because such interstitial impurities are known to influence recrystallization, grain growth, and the other related material properties due to their segregation at grain boundaries, lowering those concentrations was considered in the fabrication of materials. It is known that grain refinement leads to strengthening and toughening of most metals including W [44, 45], even if their major chemical compositions are the same. In the present study, grain size of K-doped W and K-doped W-3%Re was smaller than that of IGP pure W. Although the grain refinement was not the only factor, the ultimate tensile strength of K-doped W and K-doped W-3%Re was higher than that of IGP pure W. The further discussion on the relationship between mechanical properties and microstructure is described in section 3.

By using these materials, miniature bend-bar specimens along L-T orientation were produced by electrical discharge machining (EDM), which had 12 mm length, 1 mm width, and 1 mm thickness. The orientations of the L, T, and S directions are indicated in Fig. 1. The L, T, and S directions are the rolling direction, normal to the rolling direction, and perpendicular to both L and T directions, respectively.

2.2 Neutron irradiation

Neutron irradiation tests of the miniature bend-bar specimens made of IGP pure W, K-doped W, and K-doped W-3%Re were carried out in the Belgium Reactor 2 (BR2) of SCK·CEN in Belgium. Specimens were neutron-irradiated in BR2 up to 1.51×10^{21} n/cm^2 at 600 ºC, 1.68×10^{21} n/cm^2 at 1000 ºC, and 1.37×10^{21} n/cm^2 at 1100 ºC under fast neutron flux of approximately 8.69×10^{13} n/cm^2/s, 9.67×10^{13} n/cm^2/s, and 9.55×10^{13} n/cm^2/s, respectively, where neutron energy (E_n) above 1 MeV was considered. The values of displacement damage (unit: dpa) were 1.135 at 600 ºC, 1.245 at 1000 ºC, and 1.040 at 1100 ºC, which were calculated using MCNP6 neutronics calculation (MCNP is a general-purpose Monte Carlo N-Particle code that can be used for neutron, photon, electron, or coupled neutron/photon/electron transport.) with a threshold displacement energy (E_d) of 55 eV [46, 47]. Neutron irradiation conditions in the present study are summarized in Table 2.

As mentioned in the last section, thermal neutrons cause solid transmutation, which could induce significant irradiation hardening [22–37]. In the present neutron irradiation campaign, stainless steel thick-walled capsules were implemented to shield the W specimens from the thermal neutrons to suppress solid transmutation to a large extent. As a result, an amount of transmutation products per dpa resulted in 1.87 at.%-Re/dpa and 0.192 at.%-Os/dpa in non-alloyed W materials (i.e. in pure W and K-doped W) and 1.44 at.%-Re/dpa and 0.96 at.%-Os/dpa in W materials alloyed by Re (i.e. K-doped W-3%Re),

which was calculated by MCNP6 [47].

2.3 Post irradiation examination

In this paper, we report the results of post irradiation examination (PIE) applied to specimens irradiated at 600 ºC and 1100 ºC. The PIE of specimens irradiated at 1000 ºC is still in progress and will be reported separately.

The three point bending tests were performed in a hot-cell of SCK·CEN using a universal testing machine equipped with a furnace in air at the temperatures ranging from –50 to 600 ºC. The test set-up followed the ASTM E290 standard [48]. The span of the lower-die and diameter of three pieces of pins for this testing was 8.5 mm and 2.5 mm, respectively. The load and displacement were measured with a strain gauge load cell and an actuator, respectively. The tests were performed at a constant displacement rate with a cross-head speed of 0.723 mm/min equivalent to a flexural strain rate of 10^{-3} s^{-1} at the tension side of the specimen. In the non-irradiated condition, the tests were repeated several times at each studied test temperature. After the irradiation, one specimen per test temperature was applied to explore as many temperature points as possible.

Oxidation of specimens at 600 ºC in air remained very limited during the typical time required for the test (less than 2 h). Cross-check tests for tensile and fracture toughness were performed in vacuum and air, and the load-displacement curves were within the normal scatter. Given that oxidation may enhance the crack initiation (and propagation if tearing resistance is present), the tests performed in air should be considered as conservative compared to those done in vacuum. Hence, the estimated here DBTT values should be the same or lower if the tests would be made in vacuum.

Flexural stress (σ_f) and strain (ε_f) of the three point bending tests were calculated using the following equations;

$$\sigma_f = 3PL/2bd^2 \quad (1)$$

$$\varepsilon_f = 6Dd/L^2 \quad (2)$$

where P, D, L, b, and d were load, displacement, support span (8.5 mm), specimen width (1 mm), and specimen thickness (1 mm) [49].

After the three point bending tests, the fracture surface of the ruptured specimens was examined by scanning electron microscope (SEM) to evaluate the fracture mechanism.

3. Results and discussion

Stress-strain curves of three point bending tests are shown in Figs. 2–4. As for the non-irradiated materials, the stress-strain curves obtained at the same test conditions are simultaneously displayed in those figures. In most of the cases, the tests were halted upon the fracture of the specimens, except the K-doped W specimen irradiated at 1100 ºC and tested at 475 ºC. For this specimen, the test was stopped before the specimen fracture as the flexural strain reached 0.14 (further deformation would not provide valuable information given the scope of the present study). As mentioned later, the DBTT and strength were evaluated below a flexural strain of 0.1. Thus, the test result of K-doped W irradiated at 1100 ºC and tested at 475 ºC could be included in the evaluations.

Except the K-doped W-3%Re irradiated at 600 ºC, plastic deformation decreased with decrease in test temperature, and then, no plastic deformation was observed at test temperatures below a certain level. As for some neutron-irradiated materials, a significant increase in strain hardening was observed such that flexural strain of 0.05 was not reached even at 600 ºC.

There were several tests which exhibited the raising of flexural stress (applied load)

from the middle of plastic deformation (at around 0.1 of flexural strain), e.g., test at 375 ºC of K-doped W irradiated at 600 ºC. It was assumed that the increase in friction force between specimens and pins caused raising of flexural stress, however it was still uncertain. This is one of the reasons why the DBTT and strength were evaluated below the flexural strain of 0.1 in the present study.

Test temperature dependences of maximum flexural strain are shown in Fig. 5. For specimens that exhibited a maximum flexural strain above 0.1, the maximum flexural strain was plotted as 0.1. To determine the DBTT of each material, a Boltzmann sigmoidal function as given in the following equation was applied to the test temperature dependences of maximum flexural strain (ε_f);

$$\varepsilon_f(T) = \varepsilon_{f\_top}/(1 + \exp(C(T_{half} - T)) \quad (3)$$

where T, ε_{f_top}, C, and T_{half} were test temperature, upper shelf of maximum flexural strain, constant deduced from the fitting procedure, and temperature of the inflection point, respectively. In the present study, upper and lower shelves of maximum flexural strain were defined as 0.1 and 0. The temperature of inflection point (T_{half}) corresponds to the DBTT. This means DBTT in the present study is the temperature, where the maximum flexural strain is 0.05. This criterion was referred to the report by Lassila et al., where DBTT was defined as the three point bending test temperature at which specimens undergo a strain of 0.05 [50].

As shown in Fig. 5, ductile-to-brittle transition was clearly visualized by the fitting curves determined by Eq. (3). As for the IGP pure W irradiated at 600 ºC (see Fig. 5 (a)), DBTT could not be determined because of very limited data points. However, all data was below flexural strain of 0.05. Therefore, DBTT of this test condition was handled as above 580 ºC. As for the IGP pure W irradiated at 1100 ºC (see Fig. 5 (a)), only one data obtained

by a test at 580 ºC was at maximum flexural strain of 0.1. Therefore, DBTT of this test condition was handled as below 580 ºC. As for the K-doped W-3%Re irradiated at 600 ºC (see Fig. 5 (c)), the maximum flexural strain of all tested specimens was relatively low even after the test temperature raised and there was no clear transition of the value of maximum flexural strain. Therefore, DBTT could not be determined for this test condition. Therefore, DBTT of this test condition was handled as above 580 ºC.

DBTT and shift in DBTT (ΔDBTT), which was the change in DBTT due to neutron irradiation, were summarized in Fig. 6. DBTT of IGP pure W, K-doped W, and K-doped W-3%Re in the non-irradiated state were 145, 65, and –15 ºC, respectively. Reduction of DBTT in the non-irradiated state by K-doping and Re-addition were also observed in the previous Charpy impact test studies of the pure W (not IGP pure W but a hot-rolled pure W plate by powder metallurgy), K-doped W, W-3%Re, and K-doped W-3%Re [12–16]. In these previous studies, DBTT of the pure W, K-doped W, W-3%Re, and K-doped W-3%Re in the non-irradiated state were 550, 350, 450, and 250 ºC, respectively, which were obtained using KLST specimens along L-S orientation. According to the previous Charpy impact test studies of several kinds of steels with body-centered-cubic (BCC) crystalline structure in the non-irradiated and irradiated states, DBTT of miniaturized specimens was lower than that of full-size standard specimens, regardless of neutron irradiation [51–53]. Therefore, the results showing the lowered DBTT of the miniature bend-bar specimens in the present study compared to the KLST specimens could be caused by difference in specimen size. In addition, difference in specimen shape, including a notch, and test conditions, including a strain rate, might be possible factors. According to the previous study [40], the DBTT of IGP pure W along T-L orientation was 391 ºC, which was higher compared to that along L-S orientation (145 ºC). Most of W materials fabricated by powder metallurgy and method of forging, rolling, and swaging etc. demonstrated a specimen orientation dependence of DBTT and

fracture behavior, which were caused by the microstructural anisotropy [54–58]. As well as the previous studies, the difference in DBTT of the IGP pure W between L-S and T-L orientations could be related to the anisotropic microstructure of this material [38–40].

According to the previous studies, grain refinement as well as solid solution softening/ strengthening by both K-doping and alloying by Re, respectively, could be the factors related to the reduction of DBTT [13–16]. Yin et al. reported that the DBTT of W based materials was decreased with an increase of a density of low angle grain boundaries (LAGBs) and that the density of LAGBs in K-doped W and K-doped W-3%Re was higher compared to the IGP pure W [40]. The LAGBs can act as dislocation sources and the grain refinement can be accompanied by the increase in dislocation sources [45]. In addition, K bubbles dispersed in K-doped W materials can suppress the removal of LAGBs during fabrication (e.g. rolling and heat treatment) because they can hinder the motion of grain boundaries and dislocations, which control grain growth. Moreover, alloying by Re is known to enhance the mobility of ½<111> screw dislocations in the low temperature region and thereby to reduce the DBTT of W-Re alloys [59]. Thus, the K-doping and alloying by Re could simultaneously act to reduce the DBTT of W, at least in the non-irradiated state.

After the neutron irradiation, DBTT of IGP pure W, K-doped W, and K-doped W-3%Re were above 580, 300, and above 580 ºC for irradiation temperature of 600 ºC and below 580, 320, and 330 ºC for irradiation temperature of 1100 ºC, respectively. As shown in Fig. 7, fracture manner of K-doped W and K-doped W-3%Re irradiated at 1100 ºC was ductile above DBTT and cleavage below DBTT. According to the previous study on Charpy impact properties in the non-irradiated state, K-doped W and K-doped W-3%Re showed as well ductile fracture above DBTT and cleavage below DBTT [13, 15, 16]. In addition, according to the previous study on long term microstructural stability at 1100 ºC in the non-irradiated state, K-doped W showed recrystallization after annealing less than 5×10^2 h,

whereas K-doped W-3%Re showed no recrystallization after annealing up to 3×10^3 h [16]. Because the total irradiation time in the present study was 166 days, which is approximately 4×10^3 h, K-doped W is certainly expected to undergo certain degree of recrystallization purely due to thermal exposure. In the case of K-doped W-3%Re, the thermal exposure during the irradiation time should not cause the recrystallization. Based on these experimental results, no change in the fracture manner occurred even due to the combined effect of neutron irradiation damage and long-term annealing accompanied by recrystallization.

As shown in the table in Fig. 6, DBTT shift of those materials was above 435, 235, and above 595 ºC for irradiation temperature of 600 ºC and below 435, 255, and 345 ºC for irradiation temperature of 1100 ºC, respectively. K-doped W demonstrated the suppressed neutron-irradiation-induced embrittlement, regardless of irradiation temperatures. In contrast, K-doped W-3%Re also demonstrated the suppressed embrittlement at the irradiation temperature of 1100 ºC, however no positive effect was observed at the irradiation temperature of 600 ºC. From the viewpoint of shift in DBTT, K-doping might be more effective than alloying by Re to suppress neutron-irradiation-induced embrittlement. As mentioned above, the neutron irradiation fluence in the present study reached a level, where the solid transmutation was no longer negligible. The total transmutation in K-doped W-3%Re was higher than in other two studied materials (due to transmutation of Re to Os by absorption of thermal neutrons). Therefore, in the case of K-doped W, a smaller concentration of transmutation products resulted in the lower irradiation hardening and lower DBTT shift.

As mentioned above, K-doped W-3%Re irradiated at 600 ºC exhibited no clear DBTT with relatively low maximum flexural strain below the test temperature of 580 ºC, whereas that irradiated at 1100 ºC exhibited no such behavior. This difference might be attributed to high temperature stability of W-Re-Os clusters and precipitates attributed to the solid transmutation. Hu et al. investigated the high temperature stability of W-Re-Os clusters

and precipitates in single-crystal W produced by neutron irradiation in HFIR, where relatively higher amount of solid transmutation products formed in W due to relatively higher ratio of thermal neutrons [35]. According to this report, neutron irradiation at 705 ºC produced a homogeneous distribution of W-Re-Os clusters, while such clusters dissolved by post-irradiation annealing at 1200 ºC for 2 h. Therefore, temperature of 1200 ºC seemed to be high enough to drive the dissociation of W-Re-Os alloys. In contrast, neutron irradiation at 1100 ºC produced sparse distribution of precipitates enriched in Re and Os, which could indicate high temperature stability of precipitates at this temperature [35]. However, in this case, Os was more concentrated, while Re was more dissolved. In addition, some of the visible precipitates were only enriched in Os, while the segregation of Re around the precipitates was not obvious. Based on these experimental results, dissolving the W-Re-Os clusters during high temperature irradiation, and chemical composition, shape, number density, and distribution of precipitates enriched in Re and Os were considered to cause the difference in embrittlement behavior of K-doped W-3%Re, which was dependent on the neutron irradiation temperature. To clarify the mechanism of embrittlement behavior, microstructural study is planned as a further PIE within the present study.

Fig. 8 shows the test temperature dependences of maximum flexural stress, when the flexural strain was limited less than 0.1 (hereafter, it is called as "flexural stress limited to 0.1 strain"). For specimens that exhibited a maximum flexural strain above 0.1, the flexural stress limited to 0.1 strain was plotted as that at the flexural strain of 0.1. For specimens that exhibited a maximum flexural strain below 0.1, the flexural stress limited to 0.1 strain was plotted as that at the maximum flexural strain. The flexural stress limited to 0.1 strain in the non-irradiated state decreased with test temperature, regardless of materials. In addition, the flexural stress limited to 0.1 strain of K-doped W and K-doped W-3%Re was higher compared to pure W. These tendencies were consistent with test temperature dependence of

tensile strength of those materials [5, 6, 9, 13, 15, 16, 39]. In contrast to the non-irradiated state, K-doped W irradiated at 600 and 1100 ºC and K-doped W-3%Re irradiated at 1100 ºC exhibited almost no change in the flexural stress limited to 0.1 strain at temperature range of the upper shelf of maximum flexural strain, and decrease in the flexural stress limited to 0.1 strain with decrease in test temperature below the lower temperature limit of upper shelf of maximum flexural strain. Although the irradiation-induced microstructure, hardening behavior, and effect of test temperature might affect these behaviors, it was still uncertain. Further fractography and microstructural study are planned within the present study to clarify that.

The upper and lower limits of operation temperature of fusion reactor components using W materials, such as the divertor, would be determined by the recrystallization temperature and DBTT, respectively. Therefore, higher recrystallization temperature, lower DBTT, and their suppressed changes by neutron irradiation are desirable. According to the previous studies on microstructural stability against isochronal annealing for 1 h [12, 13, 15, 16], recrystallization temperature of pure W, K-doped W, and K-doped W-3%Re in the non-irradiated state was 1250, 1350, and 1450 °C, respectively. In addition, according to the previous study on long term microstructural stability at 1100 ºC in the non-irradiated state, pure W and K-doped W showed recrystallization after annealing less than 1×10^2 h and less than 5×10^2 h, respectively, whereas K-doped W-3%Re showed no recrystallization after annealing up to 3×10^3 h [16]. Based on the results obtained in the present and previous studies (DBTT in non-irradiated state, shift in DBTT due to the irradiation, and recrystallization temperature), K-doped W-3%Re offered the best performance for applications of fusion reactor, if considering only properties in the non-irradiated state. If one accounts for the neutron irradiation up to approximately 0.5 dpa, which was accompanied by no or very small amount of solid transmutation, this material could still show insignificant

degradation of mechanical properties, according to the previous neutron irradiation studies [17, 18]. However, if the neutron irradiation reaches a level, where the amount of solid transmutation products is no longer negligible, the neutron-irradiation-induced embrittlement may become an intrinsic concern for the W based materials. The embrittlement could be mainly caused by the formation of the irradiation induced/enhanced precipitation and solute-rich clusters. Especially, because W based materials alloyed by Re, such as K-doped W-3%Re, generate higher amount of solid transmutation products compared to non-alloyed materials, further significant embrittlement might occur, as shown by the result of K-doped W-3%Re irradiated at 600 ºC up to 1.135 dpa in the present study. As mentioned in section 2.2, the amount of transmutant Re and Os produced in K-doped W-3%Re was approximately 30% and 20% higher compared to pure W and K-doped W. Based on this discussion, the investigation of the thermo-mechanical properties, especially under extended neutron irradiation fluence attained at various temperatures, is necessary to clarify the effectiveness of alloying by Re. In contrast, K-doped W exhibited several improvements in terms of thermo-mechanical properties in the non-irradiated state as compared to pure W from the previous studies [5, 6, 11, 13, 15–18], and also demonstrated a better resistance (compared to IGP pure W or K-doped W-3%Re) against neutron irradiation in the present study. Therefore, K-doping could be considered as one of the effective modification methods of W based materials for application to future fusion reactor components accompanied by a long-term operation.

4. Summary and conclusions

The effect of neutron irradiation on the mechanical properties of K-doped W and K-doped W-3%Re plates, fabricated by powder metallurgy and hot-rolling, was investigated to clarify tolerance and susceptibility of these new W grades to the irradiation. Together with

these materials, IGP pure W was irradiated face-to-face and examined to assess the effect of K-doping and alloying by Re. The miniature bend-bar specimens made of those three materials were exposed to neutron irradiation in BR2 reactor of SCK·CEN in Belgium up to 1.135 dpa at 600 ºC, up to 1.245 dpa at 1000 ºC, and up to 1.040 dpa at 1100 ºC. In the present neutron irradiation campaign, the irradiation fluence reached a level, where the solid transmutation was no longer negligible. Three point bending tests of the specimens irradiated at 600 ºC and 1100 ºC were performed at the temperatures ranging from –50 to 600 ºC to investigate the neutron-irradiation-induced embrittlement on the resulting flexural stress and strain. The results of the present study were summarized as follows:

(1) DBTT of IGP pure W, K-doped W, and K-doped W-3%Re in the non-irradiated state was found to be 145, 65, and –15 ºC, respectively. The followings were considered as possible factors for the reduction of DBTT in the modified materials: (i) a grain refinement by both K-doping and Re-addition; (ii) an enhancement of LAGBs density, acting as sources of dislocations; (iii) stabilization of grain boundary interfaces by K bubbles during material fabrication; (iv) and an enhancement of the mobility of dislocations by alloying by Re. Since the above-mentioned mechanism have not been actually proved, microstructural study is planned as a further PIE within the present study.

(2) Irradiation-induced DBTT shift (change in DBTT due to the neutron irradiation) of IGP pure W was above 435 and below 435 ºC for irradiation temperatures of 600 and 1100 ºC, respectively.

(3) The DBTT shift of K-doped W was 235 and 255 ºC for irradiation temperatures of 600 and 1100 ºC, respectively. K-doped W exhibited the highest resistance (i.e. the lowest DBTT shift) to the neutron-irradiation-induced embrittlement among the materials examined in the present study.

(4) The DBTT shift of K-doped W-3%Re was above 595 and 345 ºC for irradiation temperatures of 600 and 1100 ºC, respectively. Such considerable difference in the DBTT shift can be explained by the formation/precipitation of W-Re-Os clusters under irradiation at 600 ºC, which otherwise is reduced due to thermally enhanced dissolution at 1100 ºC.

(5) According to the previous studies involving the non-irradiated materials and neutron irradiation up to 0.5 dpa, K-doped W-3%Re demonstrated a superior performance compared to pure W and K-doped W. However, the present study clarified that the neutron-irradiation-induced embrittlement (i.e. an increase in DBTT) may become an intrinsic concern of W based materials alloyed by Re above certain neutron fluence due to the solid transmutation. As a result, the Re-free K-doped W material exhibited a considerably lower DBTT shift compared to the K-doped W-3%Re irradiated up to ~1 dpa at 600 °C.

Acknowledgements

This work has been carried out within the framework of the EUROfusion Consortium and has received funding from the Euratom research and training programme 2014–2018 and 2019–2020 under grant agreement No 633053. The views and opinions expressed herein do not necessarily reflect those of the ITER Organization or of the European Commission. This work was also supported by JSPS KAKENHI Grant Number 15KK0224, 26289351, 24246151, 17H01364, and 18H01196 in Japan. In addition, this work was performed with the support and under the auspices of the National Institute for Fusion Science (NIFS) Collaboration Research program (NIFS11K0BF019) in Japan. Authors are also grateful to Mr. T. Takida, Mr. S. Nakabayashi, and Mr. N. Matsuda of A.L.M.T. Corp. for their support to our material development.

References

[1] J. M. Steichen, J. Nucl. Mater. **60** (1976) 13–19.

[2] P. Krautwasser, H. Derz, E. Kny, Proc. 12th International PLANSEE Seminar (1989) 673–681.

[3] L. M. Garrison, Y. Katoh, N. A. P. Kiran Kumar, J. Nucl. Mater. **518** (2019) 208–225.

[4] R. G. Abernethy, J. S. K. -L. Gibson, A. Giannattasio, J. D. Murphy, O. Wouters, S. Bradnam, L. W. Packer, M. R. Gilbert, M. Klimenkov, M. Rieth, H. -C. Schneider, C. D. Hardie, S. G. Roberts, D. E. J. Armstrong, J. Nucl. Mater. **527** (2019) 151799.

[5] M. Fukuda, S. Nogami, K. Yabuuchi, A. Hasegawa, T. Muroga, Fus. Sci. Technol. **68** (2015) 690–693.

[6] K. Sasaki, K. Yabuuchi, S. Nogami, A. Hasegawa, J. Nucl. Mater. **461** (2015) 357–364.

[7] S. Nogami, W. H. Guan, M. Fukuda, A. Hasegawa, Fus. Eng. Des. **109–111** (2016) 1549–1553.

[8] W. H. Guan, S. Nogami, M. Fukuda, A. Hasegawa, Fus. Eng. Des. **109–111** (2016) 1538–1542.

[9] M. Fukuda, T. Tabata, A. Hasegawa, S. Nogami, T. Muroga, Fus. Eng. Des. **109–111** (2016) 1674–1677.

[10] S. Nogami, W. H. Guan, A. Hasegawa, M. Fukuda, Fus. Sci. Technol. **72** (2017) 673–679.

[11] M. Fukuda, A. Hasegawa, S. Nogami, Fus. Eng. Des. **132** (2018) 1–6.

[12] S. Nogami, S. Watanabe, J. Reiser, M. Rieth, S. Sickinger, A. Hasegawa, Fus. Eng. Des. **135** (2018) 196–203.

[13] S. Nogami, S. Watanabe, J. Reiser, M. Rieth, S. Sickinger, A. Hasegawa, Fus. Eng. Des. **140** (2019) 48–61.

[14] S. Watanabe, S. Nogami, J. Reiser, M. Rieth, S. Sickinger, S. Baumgärtner, T. Miyazawa,

A. Hasegawa, Fus. Eng. Des. **148** (2019) 111323.

[15] S. Nogami, A. Hasegawa, M. Fukuda, S. Watanabe, J. Reiser, M. Rieth, Fus. Eng. Des. **152** (2020) 111445.

[16] S. Nogami, A. Hasegawa, M. Fukuda, M. Rieth, J. Reiser, G. Pintsuk, J. Nucl. Mater. **543** (2021) 152506.

[17] T. Miyazawa, L. M. Garrison, J. W. Geringer, M. Fukuda, Y. Katoh, T. Hinoki, A. Hasegawa, J. Nucl. Mater. **529** (2020) 151910.

[18] T. Miyazawa, L. M. Garrison, J. W. Geringer, J. R. Echols, M. Fukuda, Y. Katoh, T. Hinoki, A. Hasegawa, J. Nucl. Mater. **542** (2020) 152505.

[19] L. M. Garrison, Y. Katoh, J. W. Geringer, M. Akiyoshi, X. Chen, M. Fukuda, A. Hasegawa, T. Hinoki, X. Hu, T. Koyanagi, E. Lang, M. McAlister, J. McDuffee, T. Miyazawa, C. Parish, E. Proehl, N. Reid, J. Robertson, H. Wang, Fus. Sci. Technol. **75** (2019) 499–509.

[20] H. Bolt, V. Barabash, G. Federici, J. Linke, A. Loarte, J. Roth, K. Sato, J. Nucl. Mater. **307–311** (2002) 43–52.

[21] H. Bolt, V. Barabash, W. Krauss, J. Linke, R. Neu, S. Suzuki, N. Yoshida, ASDEX Upgrade Team, J. Nucl. Mater. **329–333** (2004) 66–73.

[22] M. Fukuda, T. Tanno, S. Nogami, A. Hasegawa, Mater. Trans. **53** (2012) 2145–2150.

[23] M. Fukuda, K. Yabuuchi, S. Nogami, A. Hasegawa, T. Tanaka, J. Nucl. Mater. **455** (2014) 460–463.

[24] M. Fukuda, N. A. P. Kiran Kumar, T. Koyanagi, L. M. Garrison, L. L. Snead, Y. Katoh, A. Hasegawa, J. Nucl. Mater. **479** (2016) 249–254.

[25] T. Tanno, A. Hasegawa, J. -C. He, M. Fujiwara, S. Nogami, M. Satou, T. Shishido, K. Abe, Mater. Trans. **48-9** (2007) 2399–2402.

[26] T. Tanno, A. Hasegawa, M. Fujiwara, J. -C. He, S. Nogami, M. Satou, T. Shishido, K.

Abe, Mater. Trans. **49-10** (2008) 2259–2264.

[27] T. Tanno, A. Hasegawa, J. -C. He, M. Fujiwara, M. Satou, S. Nogami, K. Abe, T. Shishido, J. Nucl. Mater. **386–388** (2009) 218–221.

[28] A. Hasegawa, T. Tanno, S. Nogami, M. Satou, J. Nucl. Mater. **417** (2011) 491–494.

[29] A. Hasegawa, M. Fukuda, S. Nogami, K. Yabuuchi, Fus. Eng. Des. **89** (2014) 1568–1572.

[30] A. Hasegawa, M. Fukuda, K. Yabuuchi, S. Nogami, J. Nucl. Mater. **471** (2016) 175–183.

[31] T. Hwang, A. Hasegawa, K. Tomura, N. Ebisawa, T. Toyama, Y. Nagai, M. Fukuda, T. Miyazawa, T. Tanaka, S. Nogami, J. Nucl. Mater. **507** (2018) 78–86.

[32] Y. Katoh, L. L. Snead, L. M. Garrison, X. Hu, T. Koyanagi, C. M. Parish, P. D. Edmondson, M. Fukuda, T. Hwang, T. Tanaka, A. Hasegawa, J. Nucl. Mater. **520** (2019) 193–207.

[33] X. Hu, T. Koyanagi, M. Fukuda, Y. Katoh, L. L. Snead, B. D. Wirth, J. Nucl. Mater. **470** (2016) 278–289.

[34] X. Hu, T. Koyanagi, M. Fukuda, N. A. P. Kiran Kumar, L. L. Snead, B. D. Wirth, Y. Katoh, J. Nucl. Mater. **480** (2016) 235–243.

[35] X. Hu, C. M. Parish, K. Wang, T. Koyanagi, B. P. Eftink, Y. Katoh, Acta Mater. **165** (2019) 51–61.

[36] T. Koyanagi, N. A. P. Kiran Kumar, T. Hwang, L. M. Garrison, X. Hu, L. L. Snead, Y. Katoh, J. Nucl. Mater. **490** (2017) 66–74.

[37] M. Klimenkov, U. Jäntsch, M. Rieth, H. C. Schneider, D. E. J. Armstrong, J. Gibson, S. G. Roberts, Nucl. Mater. Energy **9** (2016) 480–483.

[38] C. Yin, D. Terentyev, T. Pardoen, R. Petrov, Z. Tong, Mater. Sci. Eng. A **750** (2019) 20–30.

[39] C. Yin, D. Terentyev, T. Pardoen, A. Bakaeva, R. Petrov, S. Antusch, M. Rieth, M.

Vilémová, J. Matějíček, T. Zhang, Int. J. Refract. Met. Hard Mater. **75** (2018) 153–162.

[40] C. Yin, D. Terentyev, T. Zhang, S. Nogami, S. Antusch, C. Chang, R. H. Petrov, T. Pardoen, Int. J. Refract. Met. Hard Mater. **95** (2021) 105464.

[41] A. Dubinko, D. Terentyev, A. Bakaeva, K. Verbeken, M.Wirtz, M. Hernández-Mayoral, Int. J. Refract. Met. Hard Mater. **66** (2017) 105–115.

[42] M. Wirtz, J. Linke, Th. Loewenhoff, G. Pintsuk, I. Uytdenhouwen, Phys. Scr. **T167** (2016) 014015.

[43] ASTM E112–85, Standard Methods for Determining the Average Grain Size, Annual Book of ASTM, 1986, 227–290.

[44] K. Farrell, A. C. Schaffhauser, J. O. Stiegler, J. Less-Common Met. **13** (1967) 141–155.

[45] C. Bonnekoh, A. Hoffmann, J. Reiser, Int. J. Refract. Met. Hard Mater. **71** (2018) 181–189.

[46] S. L. Dudarev, DPA Definition and Estimates, (2015), https://www-amdis.iaea.org/CRP/IrradiatedTungsten/RCM2/RCM2Presentation-Dudarev DPA-2015-09-10.pdf.

[47] https://mcnp.lanl.gov/

[48] ASTM E290-14, Standard Test Methods for Bend Testing of Material for Ductility, ASTM international, 2014.

[49] ASTM D790-17, Standard Test Methods for Flexural Properties of Unreinforced and Reinforced Plastics and Electrical Insulating Materials, ASTM international, 2017.

[50] D. H. Lassila, F. Magness, D. Freeman, Ductile-Brittle Transition Temperature Testing of Tungsten Using the Three-Point Bend Test, Report Lawrence Livermore National Laboratory UCRL-ID-108258 (1991).

[51] W. R. Corwin, R. L. Klueh, J. M. Vitek, J. Nucl. Mater. **122** (1984) 343–348.

[52] L. E. Schubert, A. S. Kumar, S. T. Rosinki, M. L. Hamilton, J. Nucl. Mater. **225** (1995)

231–237.

[53] B. S. Louden, A. S. Kumar, F. A. Garner, M. L. Hamilton, W. L. Hu, J. Nucl. Mater. **155–157** (1988) 662–667.

[54] M. Rieth, A. Hoffmann, Advances in Science and Technology **59** (2008) 101–104.

[55] D. Rupp, S. M. Weygand, Phil. Mag. **90** (2010) 4055–4069.

[56] D. Rupp, S. M. Weygand, J. Nucl. Mater. **417** (2011) 477–480.

[57] M. Rieth, J, Reiser, B. Dafferner, S, Baumgärtner, Fus. Sci. Technol. **61** (2012) 381–384.

[58] E. Gaganidze, D. Rupp, J. Aktaa, J. Nucl. Mater. **446** (2014) 240–245.

[59] L. Romaner, C. Ambrosch-Draxl, R. Pippan, Phys. Rev. Lett. **104 (19)** (2010) 195503.

Table 1 Interstitial impurities (C, O, and N), grain sizes along L, T, and S directions (d_L, d_T, and d_S, respectively), and ultimate tensile strength at 300 and 500 ºC along L direction of IGP pure W, K-doped W, and K-doped W-3%Re [13, 15, 16, 38–42]. Grain sizes were determined by high angle grain boundaries (HAGBs) and measured based on the ASTM E112-85 standard with inverse pole figure (IPF) images obtained by electron backscatter diffraction (EBSD) analyses [43].

		IGP Pure W	K-doped W	K-doped W-3%Re
Impurity [wt. ppm]	C	<30	10	10
	O	<20	<10	<10
	N	<5	<10	<10
Grain size determined by HAGBs [μm]	d_L	116	30	33
	d_T	27	20	20
	d_S	24	11	8
Ultimate tensile strength (L.D.) [MPa]	300 ºC	580	780	780
	500 ºC	490	646	762

Table 2 Summary of neutron irradiation conditions. The values of displacement damage were calculated using MCNP6 with a threshold displacement energy (E_d) of 55 eV [46, 47].

Reactor	Capsule	Cycles	Thermal neutron flux [n/cm^2/s] (E_n < 0.1 MeV)	Fast neutron flux [n/cm^2/s] (E_n > 1 MeV)	Irradiation time [days]	Fast neutron Fluence [n/cm^2] (E_n > 1 MeV)	Displacement Damage [dpa]	Irradiation temperature [ºC]
BR2	TB01	7	3.22×10^{14}	8.69×10^{13}	201	1.51×10^{21}	1.135	600
	TB02	7	3.58×10^{14}	9.67×10^{13}	201	1.68×10^{21}	1.245	1000
	TB03	6	3.50×10^{14}	9.55×10^{13}	166	1.37×10^{21}	1.040	1100

Fig. 1 Nomenclature of directions of materials and specimens, shape and dimensions of miniature bend-bar specimen. The inverse pole figure (IPF) image obtained by electron backscatter diffraction (EBSD) analyses was for K-doped W [13].

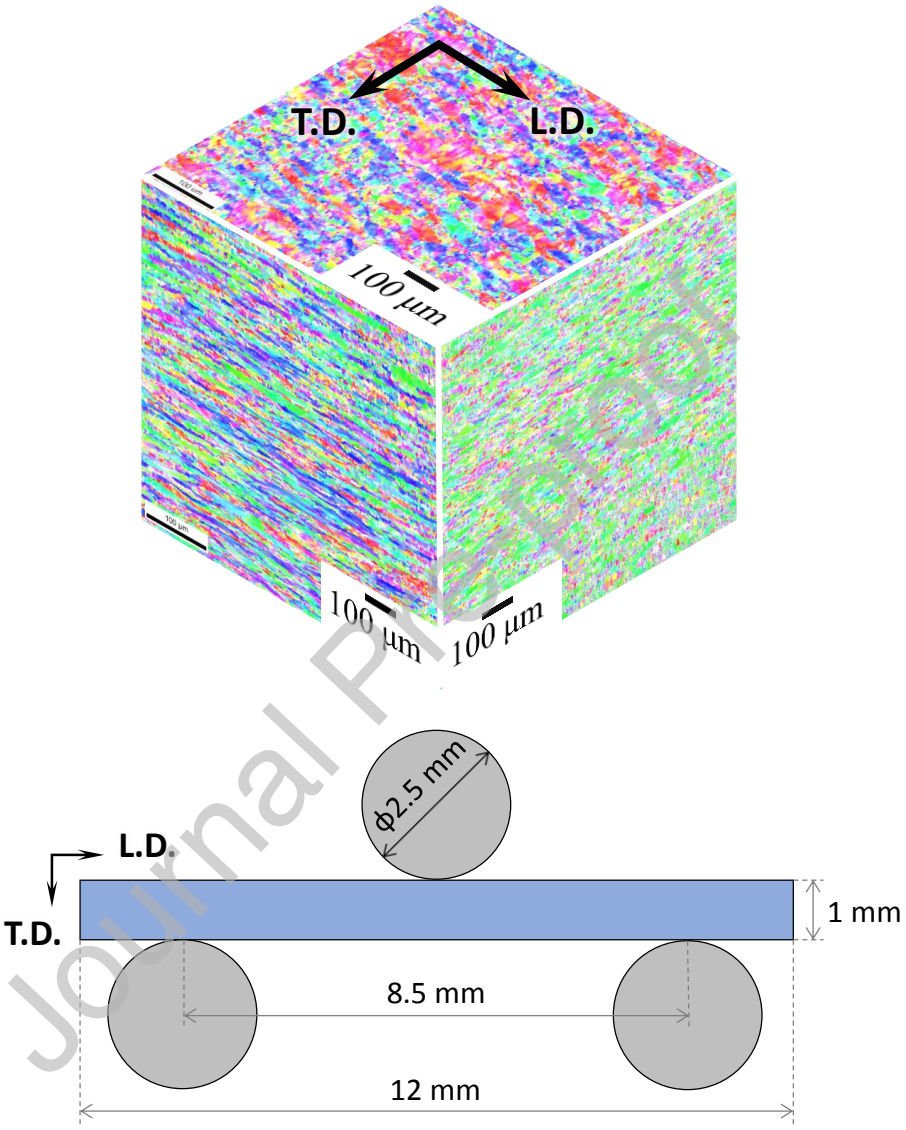

Fig. 2 Stress-strain curves of three point bending tests along L-T orientation of IGP pure W (a) in the non-irradiated state and after neutron irradiation at (b) 600 ºC up to 1.135 dpa and (c) 1100 ºC up to 1.040 dpa. Temperatures displayed in the graphs are test temperature.

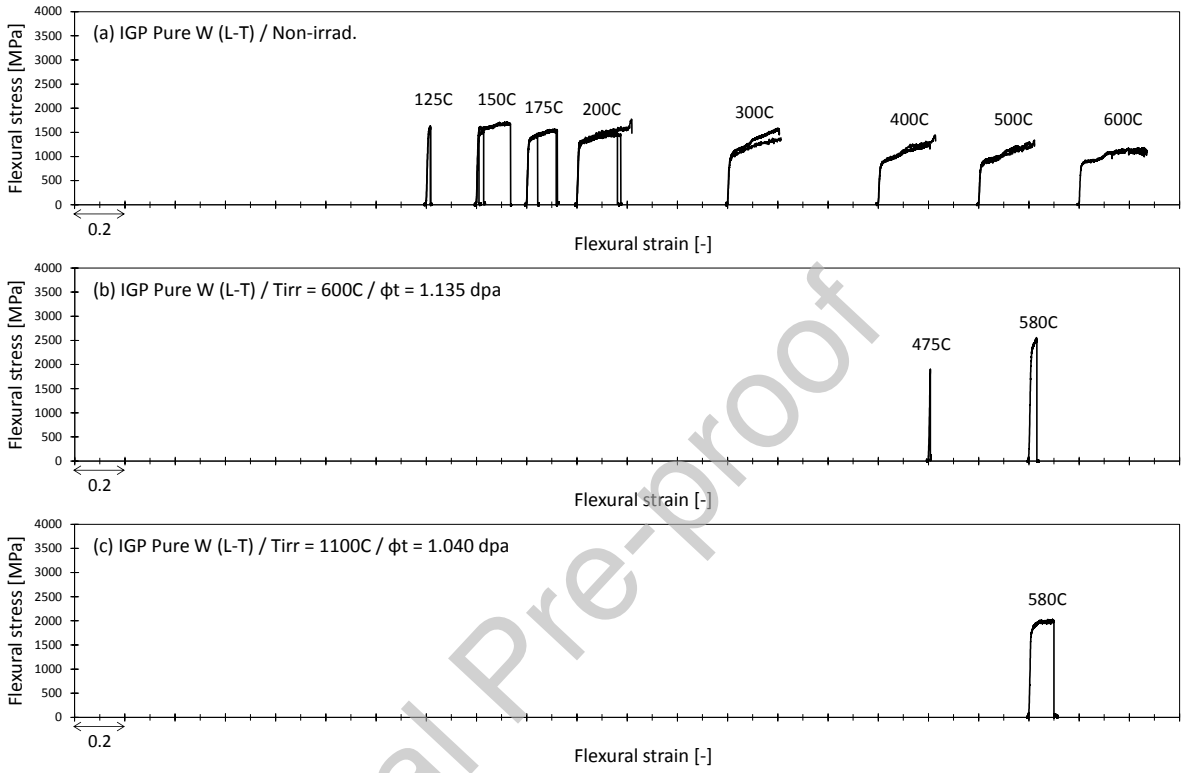

Fig. 3 Stress-strain curves of three point bending tests along L-T orientation of K-doped W (a) in the non-irradiated state and after neutron irradiation at (b) 600 ºC up to 1.135 dpa and (c) 1100 ºC up to 1.040 dpa. Temperatures displayed in the graphs are test temperature.

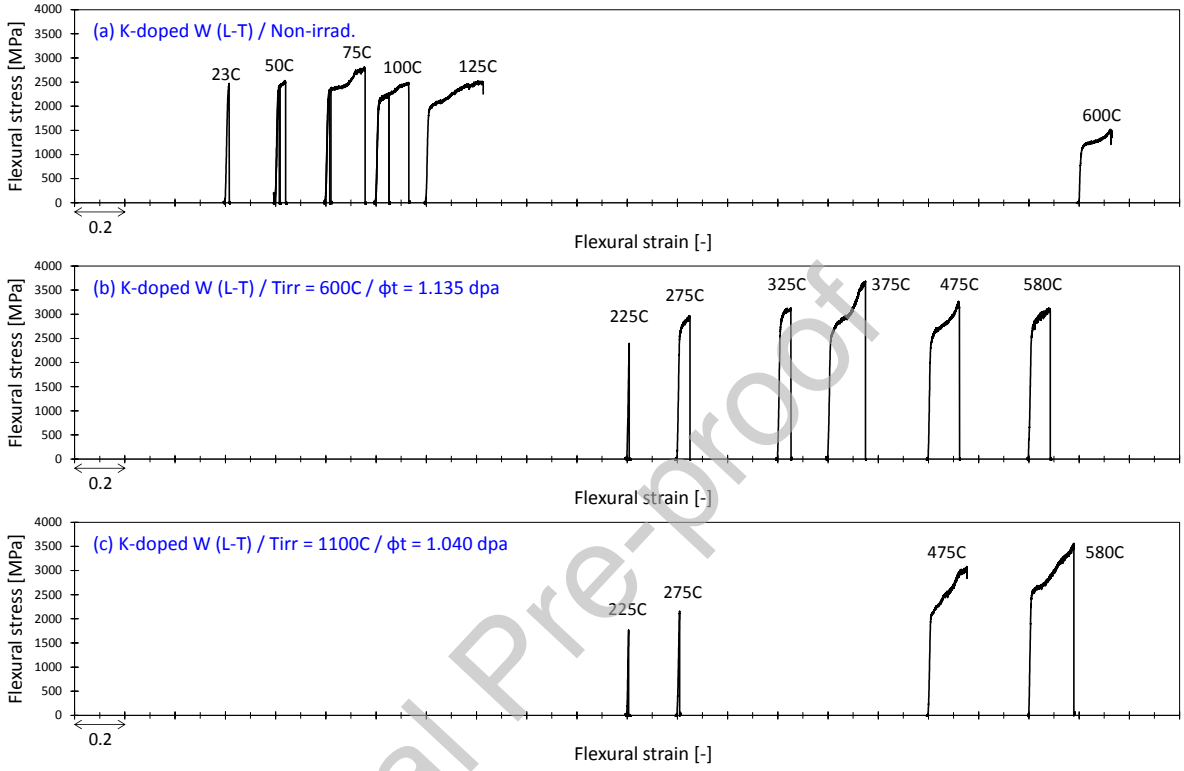

Fig. 4 Stress-strain curves of three point bending tests along L-T orientation of K-doped W-3%Re (a) in the non-irradiated state and after neutron irradiation at (b) 600 ºC up to 1.135 dpa and (c) 1100 ºC up to 1.040 dpa. Temperatures displayed in the graphs are test temperature.

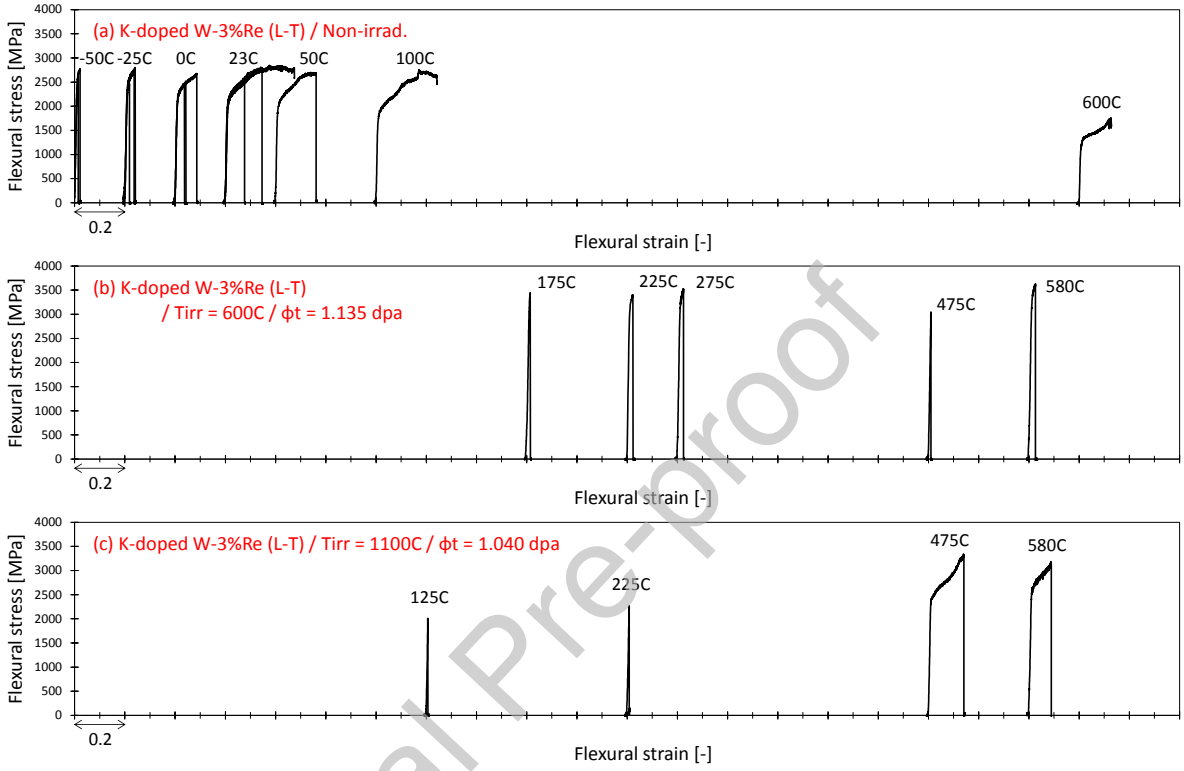

Fig. 5 Test temperature dependences of maximum flexural strain of three point bending tests along L-T orientation of (a) IGP pure W, (b) K-doped W, and (c) K-doped W-3%Re in the non-irradiated state and after neutron irradiation at 600 ºC up to 1.135 dpa and 1100 ºC up to 1.040 dpa. For specimens that exhibited a maximum flexural strain above 0.1, the maximum flexural was plotted as 0.1.

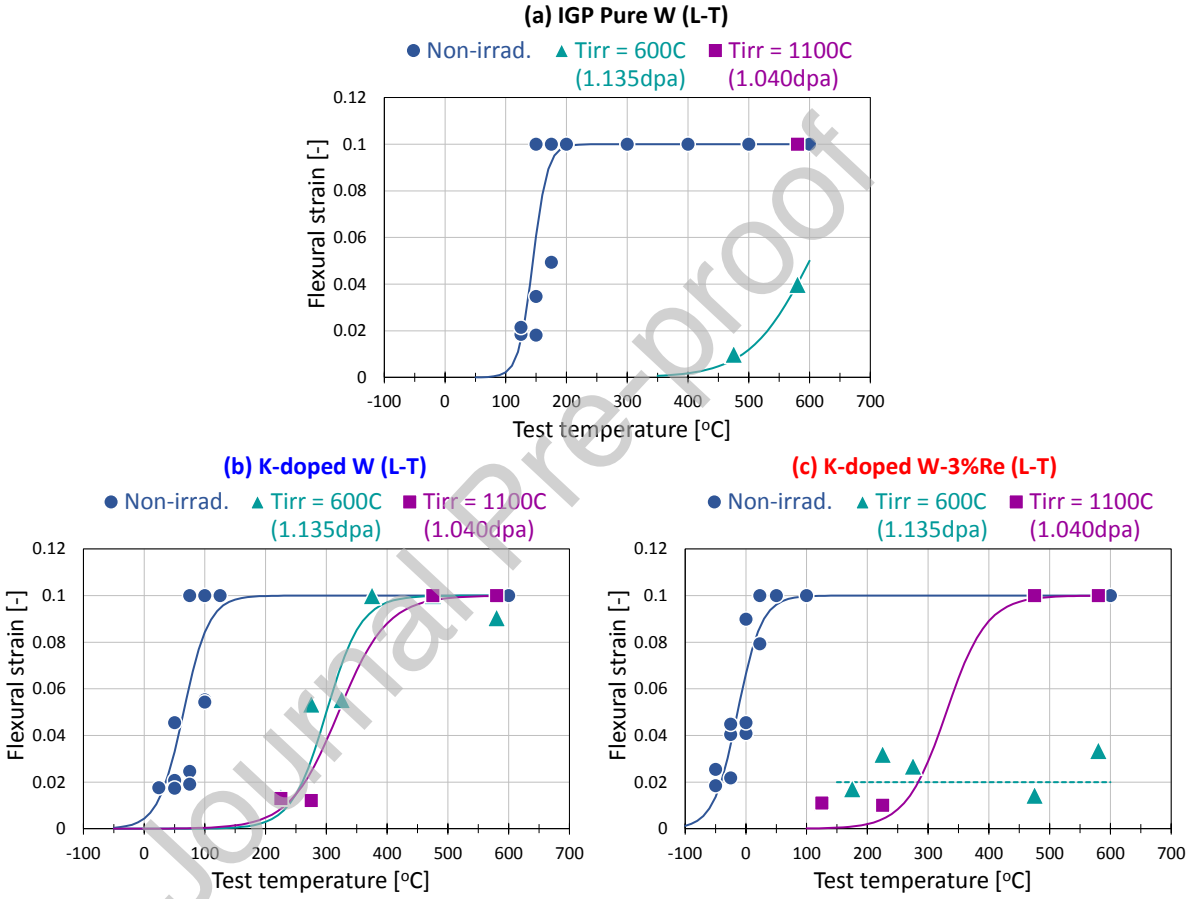

Fig. 6 DBTT and shift in DBTT (ΔDBTT) by neutron irradiation determined by test temperature dependences of maximum flexural strain of three point bend tests along L-T orientation of IGP pure W, K-doped W, and K-doped W-3%Re in the non-irradiated state and after neutron irradiation at 600 ºC up to 1.135 dpa and 1100 ºC up to 1.040 dpa.

ΔDBTT [ºC]	IGP Pure W	K-doped W	K-doped W-3%Re
T_{irr} = 600 ºC ϕt = 1.135 dpa	>435	235	>595
T_{irr} = 1100 ºC ϕt = 1.040 dpa	<435	255	345

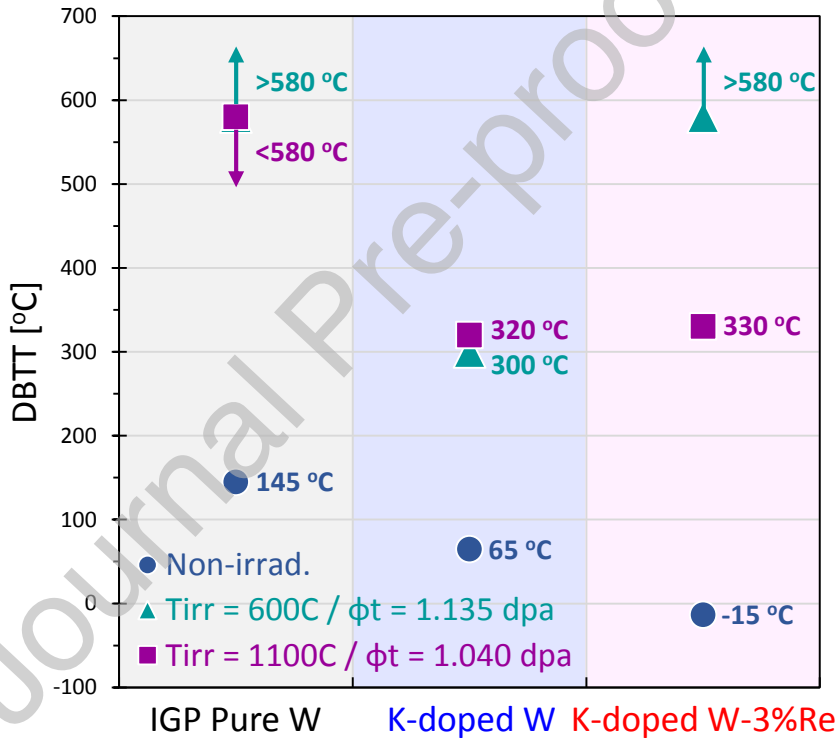

Fig. 7 Fracture surfaces of specimens after three point bending tests along L-T orientation of K-doped W tested at (a) 225 ºC and (b) 580 ºC and K-doped W-3%Re tested at (c) 125 ºC and (d) 580 ºC after neutron irradiation at 1100 ºC up to 1.040 dpa.

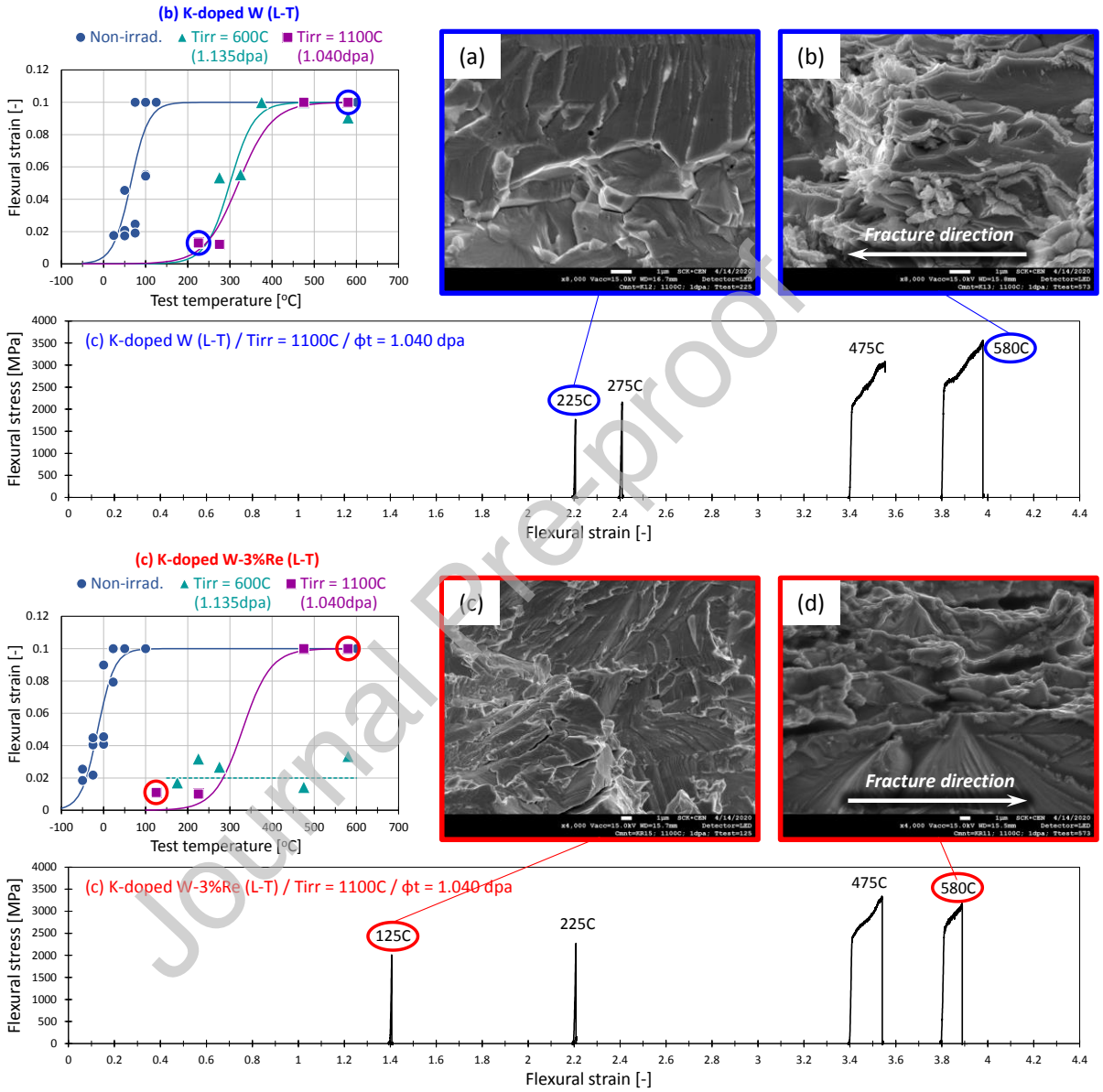

Fig. 8 Test temperature dependences of flexural stress limited to 0.1 strain of three point bending tests along L-T orientation of (a) IGP pure W, (b) K-doped W, and (c) K-doped W-3%Re in the non-irradiated state and after neutron irradiation at 600 ºC up to 1.135 dpa and 1100 ºC up to 1.040 dpa. For specimens that exhibited a maximum flexural strain above 0.1, the flexural stress limited to 0.1 strain was plotted as that at the flexural strain of 0.1. For specimens that exhibited a maximum flexural strain below 0.1, the flexural stress limited to 0.1 strain was plotted as that at the maximum flexural strain.